Egypt. J. Chem. **Vol. 67**, No.2 pp. 601 - 613 (2024)

Egyptian Journal of Chemistry

http://ejchem.journals.ekb.eg/

Synthesis of Silver Nanoparticles With Different Decoration Forms Dispersed In Nematic Liquid Crystals

Hend M. Abdulnaby [a] , I.M.Elkashef [a] , Saber Ibrahim [b] , Ahmad M. Labeeb [c]

[a]*Physics department, Faculty of science, Arish University, 45511, Arish, Egypt*

[b]*Packaging Materials Department, National Research Centre, Elbuhoth Street 33, Dokki, Cairo, 12311, Egypt*

[c] *Microwaves Physics and Dielectrics Department, Liquid crystals laboratory, Physics Research Institute, National Research Centre, Elbuhoth Street 33, Dokki, Cairo, 12311, Egypt*

Abstract

The formed lyotropic liquid crystals phases via polyvinylpyrrolidone (PVP) and cetyltrimethyl ammonium bromide (CTAB), adopting the hydrothermal and seed-mediate techniques was prepared to reduce silver nitrate (AgNO3) for shape and size controlled silver oxide nanoparticles production. Starting the reaction, PVP was coordinated with Ag+ to carry out the oxide forms of silver nanoparticles. The silver nanoparticles were characterized by UV-vis spectrometer, scanning electron microscopy (SEM), polarizing optical microscope (POM), dynamic light scattering (DLS), differential scanning calorimetry (DSC) and X-ray diffraction (XRD). Results have shown that, XRD confirmed the lattice structure of synthesized silver oxide nanoparticles. The topographic behavior of electronic surface scanning exhibits nice porous nanoparticles of silver oxide. In addition, the DSC thermal bands have a good agreement with POM transition phases. Long silver nanowires with lengths of 10-17 μm and width 0.08-2.6 μm, while the pores size of porous silver nanoparticles with varying sizes from 55 nm to 118 nm are produced. The produced nano particles in nematic cholesteric liquid crystals has significant influence on the self-assemblies of the cholesteric system.

Keyword: Nematic phase; cholesteryl benzoate; silver oxide nanoparticles; Lyotropic liquid crystals.

1. Introduction

Due to the high surface energy of nanoscale materials, coagulation and/or aggregation of nanoparticles are the major problems in the synthesis of nanoparticles globally. There are numerous uses for metal nanoparticles in numerous industries. Particularly, given that the composition, dimensions, and physical, chemical, and optical properties of metallic nanoparticles are strongly correlated [1-4]. Nanoparticles (NPs) have a high surface reactivity and a large surface-to-volume ratio [5].

Nano-sized silver has a wide range of uses in a number of industries, including health, agriculture, manufacturing, electronics, and other domains of human activity, according to the unique physical, chemical, and biological characteristics of silver [6-7]. Different types of polymers (ethylene glycol-carboxylate polystyrene beads and amidine polystyrene…etc.) [8-9] are used in synthesis of different form of silver nanoparticles.

On the other hand, liquid crystals (LCs) are soft

*Corresponding author e-mail: hendmohamed26284@yahoo.com ; (Hend M. Abdulnaby).
Received date 12 June 2023; revised date 27 July 2023; accepted date 30 July 2023.
DOI: 10.21608/EJCHEM.2023.217179.8128

materials that have a variety of intermediate phases, or mesophases. The structure exists between a disordered liquid with low symmetry and an ordered crystalline phase with high symmetry. They go through many symmetry-breaking phase transitions when the temperature drops, and they progressively develop orientational and partial positional order [10].

The liquid crystal state is between the isotropic liquid and the three-dimensionally organized crystal state. The year 1888 is associated with the discovery of liquid crystals (LCs), when Friedrich Reinitzer reported his observing of two melting points of cholesterol benzoate [11-12]. Several organic compounds show LC behavior in specific conditions. In the fused state (LC thermotropes), or in the presence of a solvent as in LC lyotropes, LC behavior can be seen [13].

There are several types of LCs, including: Nematic LCs are three-dimensional (3D) fluid phases of matter where the anisometric components of the material, such as molecules, molecular assemblies, and micelles, maintain some degree of long-range orientational order while dispersing in a form like liquids [14-15]. The word "lyotropic" was created from the words "solvent" and "forms," respectively. The concentration of water and other solvents affects how quickly the structure assembles by itself [16]. The repeating self-assembled units of lyotropic LCs, which have order over a long distance in a well-defined crystalline lattice [17]. They are further divided into cubic, hexagonal, and lamellar phases [18].

Studying nematic phase structure, chiral Nematic LCs (N*) are often used instead of the nomenclature for LCs based on cholesterol derivatives (cholesterol-based LCs, or CLC) [19]. The cholesteric liquid crystal's helical structure is made up of stacked layers with molecules arranged in an oriented order [20-23]. The least order of the director in the Nematic phase is determined by the mean direction of the mesogenic molecules or LCs which are oriented in one direction. Also, this phase responds very well to thermal and electrical influences [24].

A new challenge for researchers and a significant area of study are LC elements and the unique properties of nanoparticles [25]. Many efforts have been made to improve the electro-optical, dielectric, physico-chemical, and structural rearrangements of LCs by adding the appropriate nanoscale dopants to the host LC material. Due to their wide range of properties, metal oxide nanoparticles (MO-NPs) have recently gained a lot of interest. Researchers have successfully distributed suitable MONPs in LCs for achieving remarkable results by using their variety of characteristics [26].

In this work, we are successfully synthesized silver nanoparticles with different decoration forms such as: silver oxide nanowires and nano porous silver oxide dispersed in cholesteryl benzoate. The novelty can be considered as a new trend of combination between silver oxide Nps and cholesteryl benzoate liquid crystal, seed-mediate method is a new method for produce porous silver nanoparticles in lyotropic liquid crystals assistance.

2. Experimental

2.1 Materials:

Silver nitrate (99.0%, Sigma-Aldrich, USA), glycerin (C3H8O3, Sigma-Aldrich, USA), polyvinylpyrrolidone (PVP (C6H9NO)n, MW =40000 Da), sodium chloride (NaCl, Sigma-Aldrich, USA), Sodium Lauryl Sulphate (SLS, 85%, Loba Chemie, India), Cetyltrimethyl ammonium bromide (CTAB, C19H42BrN, Oxford), Ascorbic acid (C6H8O6, Sigma-Aldrich, USA), Cupric acetate (Cu (CH3COO)2. H2O) M.W=199.65, Cholesteryl Benzoate (98%, Acros organics, USA), dichloromethane, deionized water was used to prepare all aqueous solutions.

2.2 Hydrothermal synthesis of AgO Nanowires:

Hydrothermal synthesis methods involve crystallizing the nanomaterial at high temperature and pressure into aqueous solution [27]. In a typical synthesis, deionized water (DI) was used to prepare AgNO3 (0.02M, 15 ml), glycerin (0.12g, 5 ml), polyvinylpyrrolidone (PVP), with a molecular weight of 40000 (1g, 5 ml), and sodium chloride (NaCl), which was prepared as four different solutions in a well-dissolved form. While the other

solutions were made at standard room temperature, the PVP solution was prepared at 65°C. Glycerin solution was added to silver nitrate solution while stirring constantly. The PVP solution was added and stirred for 20 minutes to provide complete mixing after 5 to 10 minutes. Then, while continuing to stir, sodium chloride solution was added drop wise into the above solution until it was completely dissolved. The cloudy hydrosol was placed in a 50 mL Teflon-lined stainless steel autoclave and heated in an oven at 160° C for 10 hours.

The autoclave was then cooled to room temperature without air and the final product was in the form of a fluffy gray color. The precipitate was centrifuged to 40,000 rpm for 30 minutes and washed three times with deionized water and ethanol.

2.3 Seed –Mediate synthesis of Nano porous (AgO-Ag2O):

The porous silver nanoparticles will be prepared by adding the seed solution to the growth solution once using silver nitrate as a catalyst and again with copper acetate separately.

2.3.1 Preparation of seed solution:

In a typical synthesis, 50 ml of an aqueous solution containing 0.084 g of AgNO3 and 1.4g of sodium lauryl sulphate (SLS) were heated to 85 °C in a round bottom flask with three necks while being stirred continuously for 1 hour. The SLS employed as a seed solution for the synthesis of nano porous silver oxides.

2.3.2 Preparation of growth solution by using AgNO3 to catalyze the growth of silver nanoparticles:

45 mL of growth solution containing 0.2 g of AgNO3 and 1.65 g of cetyl trimethyl ammonium bromide (CTAB) was placed in a 50 mL Erlenmeyer flask. In order to catalyze the anisotropic growth of silver nanoparticles, 0.084 g of silver nitrate (AgNO3) was dissolved in 10 ml of deionized water, and 100 µl was then added to the growth solution. Finally, 0.17 g of ascorbic acid dissolved in 10 ml of deionized water, and 100µ was added to the previous solution as a light reducing agent, and then 5 ml of the seed solution was added to the growth solution. The sample used the Centrifugation at a speed of 40000 rpm for 30 minutes to collect the white precipitate, which was then washed three times with deionized water and ethanol.

2.3.3 *Preparation of growth solution by using cupric acetate to catalyze the growth of silver nanoparticles*:

45 mL of growth solution containing 0.2 g of AgNO3 and 1.65 g of cetyltrimethylammonium bromide (CTAB) was placed in a 50 mL Erlenmeyer flask. In order to catalyze the anisotropic growth of silver nanoparticles, 0.11 g of cupric acetate (Cu (CH3COO) 2. H2O) was dissolved in 10 ml of deionized water, and 100 µl was then added to the growth solution. Finally, 0.17 g of ascorbic acid dissolved in 10 ml of deionized water, and 100µ was added to the previous solution as a light reducing agent, and then 5 ml of the seed solution was added to the growth solution. Centrifugation at a speed of 40000 r/rim for 30 minutes was used to collect the precipitate, which was then washed three times with deionized water and ethanol.

2.4 Doping silver oxide nanoparticles in liquid crystal:

Silver oxide nanoparticles are prepared, and then added to liquid crystal(Cholesteryl Benzoate) by dissolving (0.1g) Cholesteryl Benzoate in Dichloromethane and adding (0.01g) silver oxide nanowires, then using ultrasonic probe to disperse nanoparticles with liquid crystal solution together, then drying them by hot stirrer and determine the phase transition by using polarizing optical microscope.

2.5 Characterization:

Characterization of the silver oxide nanoparticles was performed by ultraviolet-visible (UV-Vis) spectroscopy, using a double-beam UV-Vis spectrophotometer (Carry 100 with a tungsten-halogen light source) from 300 to 700 nm. The absorbance was scanned periodically in between. UV-Visible spectra (Jasco 770 UV spectrophotometer) were performed in National Research Center, (NRC), Giza, Egypt. The particle

size and range of particles were determined by using the dynamic light scattering (DLS). The morphology and topography of the prepared samples were analyzed using scanning electron microscopy (SEM, Quanta FEG 250, FEI). The phases and crystal structures of the prepared samples were characterized using an X-ray diffractometer (XRD) (Bruker D8, Discover Cu target, wavelength 1054A, 40Kv, 40Ma, Germany). Phase transitions were studied using a Leica DM750P (POM) polarizing microscope with two reflection and transmission options over a temperature range of 20 °C to 200 °C (LC Lab NRC). Crystallizing thermal behavior of dispersed silver oxide nanowires and nanoporous silver oxide in cholesteryl benzoate using differential scanning calorimetry (DSC) (SETRAM DSC-evo 131, scan rate 5 °C/min) studied by calculating degrees. All calculations applied to his second heating/cooling cycle.

3. Results and Discussion:

3.1. UV-VIS-IR spectrophotometer:

UV-visible absorption spectroscopy can be used to study and monitor the size of nanoparticles, and it is a critical tool in the investigation into the chemical mechanism that leads to nanoparticle synthesis [28].

The UV-Vis spectrum of AgO nanoparticles can be explained from Figure (1). The absorbance peak of silver nanoparticles have been detected in all types of prepared AgO. The AgNPs' UV-vis spectra showed a sharp peak in intensity, indicating a high yield of the synthesized AgNPs.

The peak of AgO Porous is noted at 390 nm, while the AgO-Cu porous has two small peaks at 370 nm and 420 nm as there are two shapes of AgO layered flakes and porous spherical particles in nano scale as shown later in SEM investigations. On Contrary, the nano wired AgO nanoparticles are ultra-long wire shape even in micro scale, and the correspondence on its absorbance peak is very broadening one 450-600 nm as well as spherical or flakes as shown at 270 nm, 330 nm and 400nm.

3.2 Dynamic light scattering (DLS) (Particle size distribution):

In the case of solution-state Brownian motions, the dynamic light scattering (DLS) method is a special characterization tool for determining the particle size and hydrodynamic radii29. As shown in Figure (2), particle size distribution of silver oxide nanowires and porous silver oxide nanoparticles are dispersed

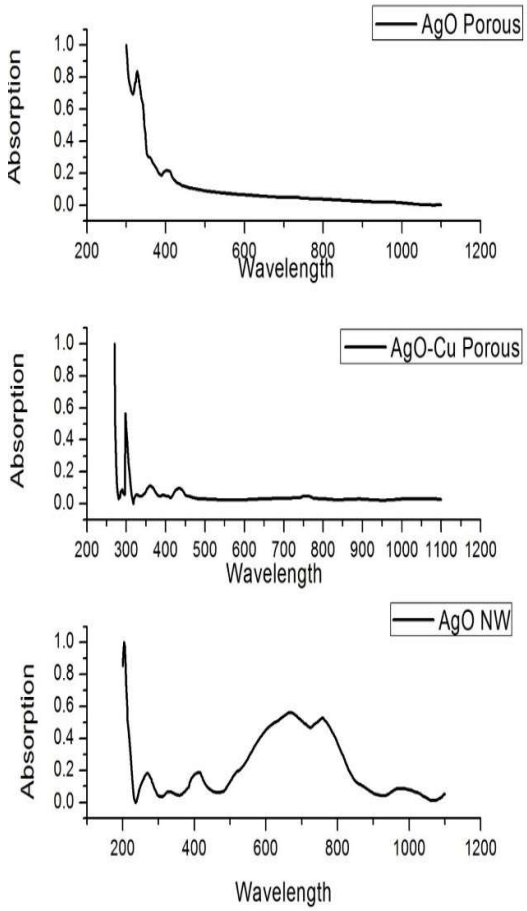

Fig. 1. UV–Vis absorbance spectra of AgNPS, AgNW and AgNPS Cu

in aqueous medium. The size distribution is well fitted by Gaussian distribution equation which its mean is around 300 nm. The reason for this mean value is the DLS technique is blindly detect the size in Brownian motion of solids content in liquids and in regardless to the direction and position of particles in front of incident laser beams before scattering, Figure (2) shows that: with a percentage of more than 90% of particles' total volume distribution, the

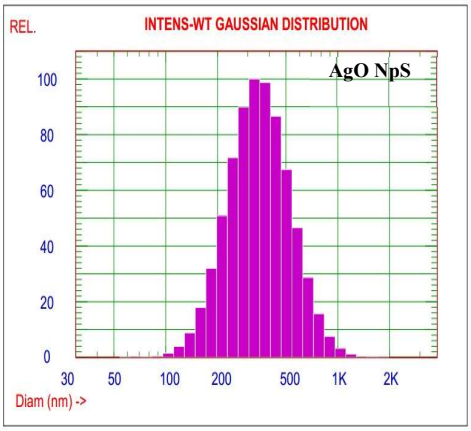

relative particle diameter measurement distribution from the range (50 - 1K) nm is presented.

Low polydispersity, or a limited distribution of silver oxide nanoparticle particle sizes, showed a homogenized distribution for those particles. The average diameter of nanoparticles was measured at 170° by dynamic light scattering (DLS) (NICOMP 380 ZLS, PSS, Santa Barbara, CA, USA).

3.3 Polarizing optical microscope (POM).

3.3.1. POM images for silver nanoparticles before doping in liquid crystal:

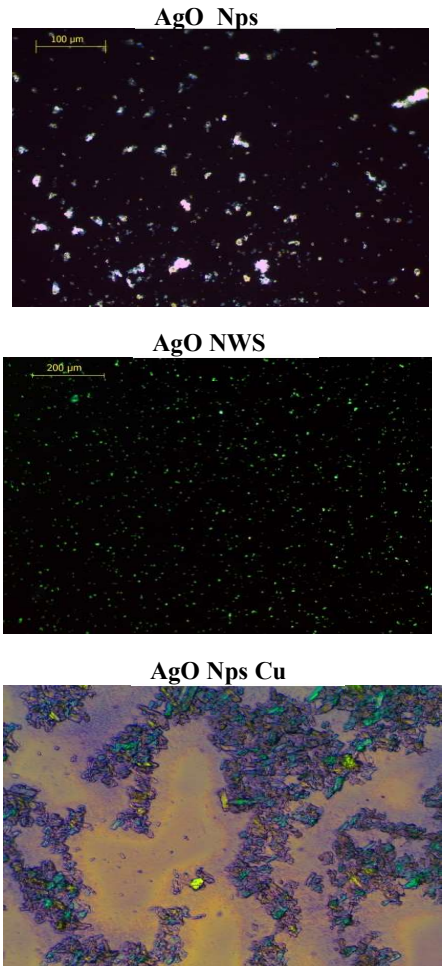

Fig. 3. The POM images of silver oxide nanoparticles

Phase transitions were studied using an equipped Leica DM750P (POM) polarizing microscope with two reflection and transmission modes over a

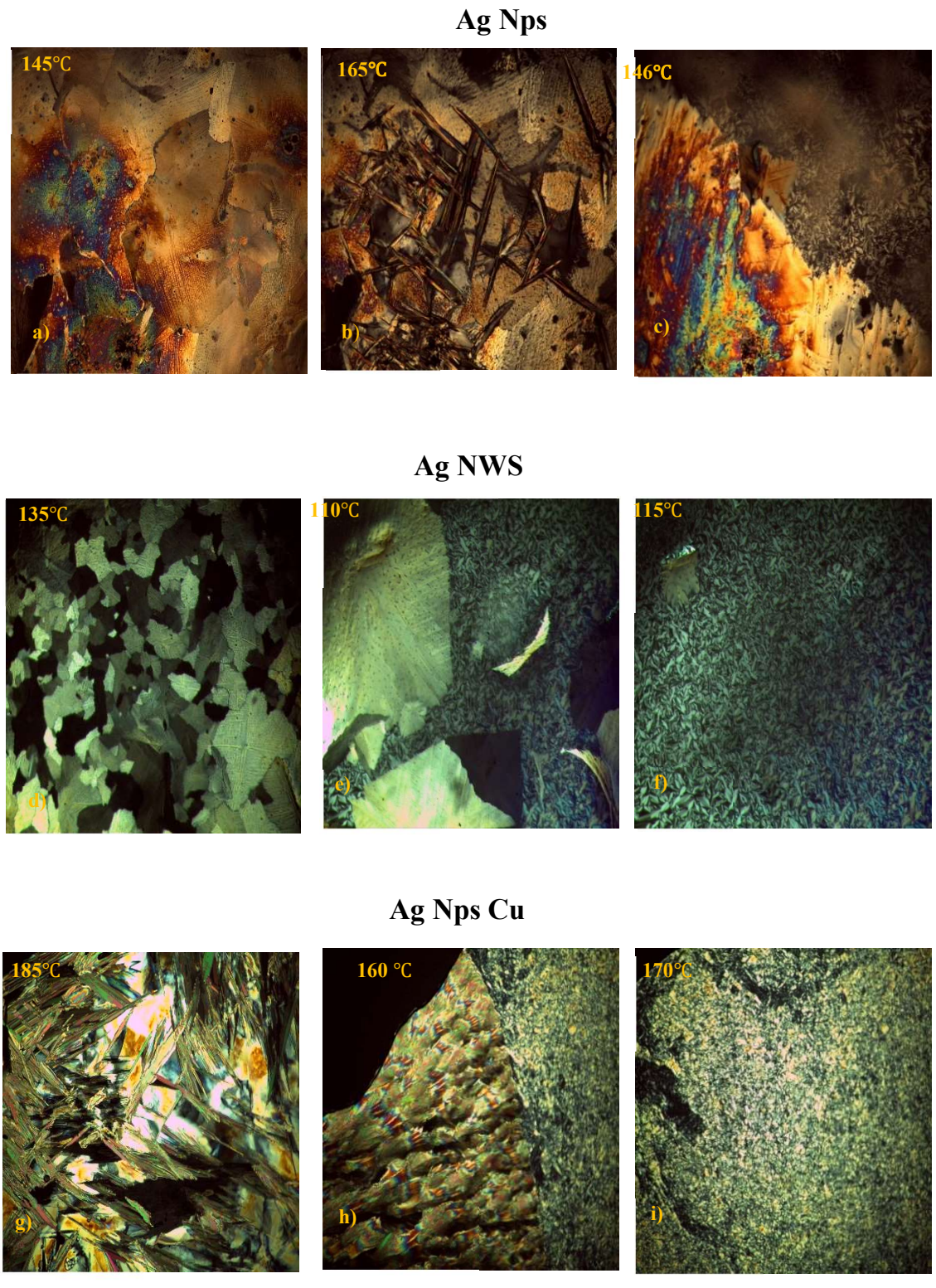

Fig. 4. POM images of Porous AgNPs-Ag NWS-Porous AgNPs Cu in presence of (CB) liquid crystal.

temperature range of 20 °C to 200 °C (LCs Lab NRC). The dispersion of lyotropic phases including inside the AgO particle graph in the left hand figure as shown in Fig.3. In the middle figure the dispersed nano wired AgO particles are shown in middle of isotropic media which appeared as black under POM microscope. Finally in the right hand, the figure is showing porous flakes of Ago NPs, the purple colour is produced due to using filter 530nm for detecting shape and size AgO texture before inserting them in LCs system.

3.3.2. POM images for silver nanoparticles after doping in liquid crystal:

The porous silver Nps dispersions in the cholesteryl benzoate (CB) liquid crystal were investigated under crossed polarizers in the POM at 10x magnification, with weight ratios of 0.1% and 1.0% wt. /wt.

AgO Nps are doping in (CB), respectively. Figure (4) demonstrated the optical textures produced by silver oxide nanoparticles: (a) First phase transition, (b) the alignment of LC molecules through AgO Nps and second phase transition occurs during heating, (c) phase transition in cooling, the top part represents fan-shaped nematic texture of liquid crystal, but the bottom part represents a crystallization.(d) first phase transition of Ag NWS dispersed in (CB), (e) the fan-shaped texture of (CB), the texture changes during the transition was rather subtle and sometimes hard to observe when cooling. (f) First phase transition in cooling cycle. (g) The distortion in color here according to the presence of copper. (h) The phase transition is clearly visible (i) the cholesteric phase growing at higher temperature. The variety in phase transition temperature according to different form of AgO NPs and weight of the sample affect the orientation.

3.4 X-rays diffraction:

AgO nanoparticles were characterized by using XRD (Bruker D8 Discover) with Cu target (λ of 1.54 Å, 40Kv, 40m A, Germany). The XRD pattern of Ag_2O nanoparticles shows the presence of Ag, AgO and Ag_2O in the sample. Nano crystalline nature of the sample confirmed by broadness of XRD spectra. Figure (5a) shows seven peaks observed at the

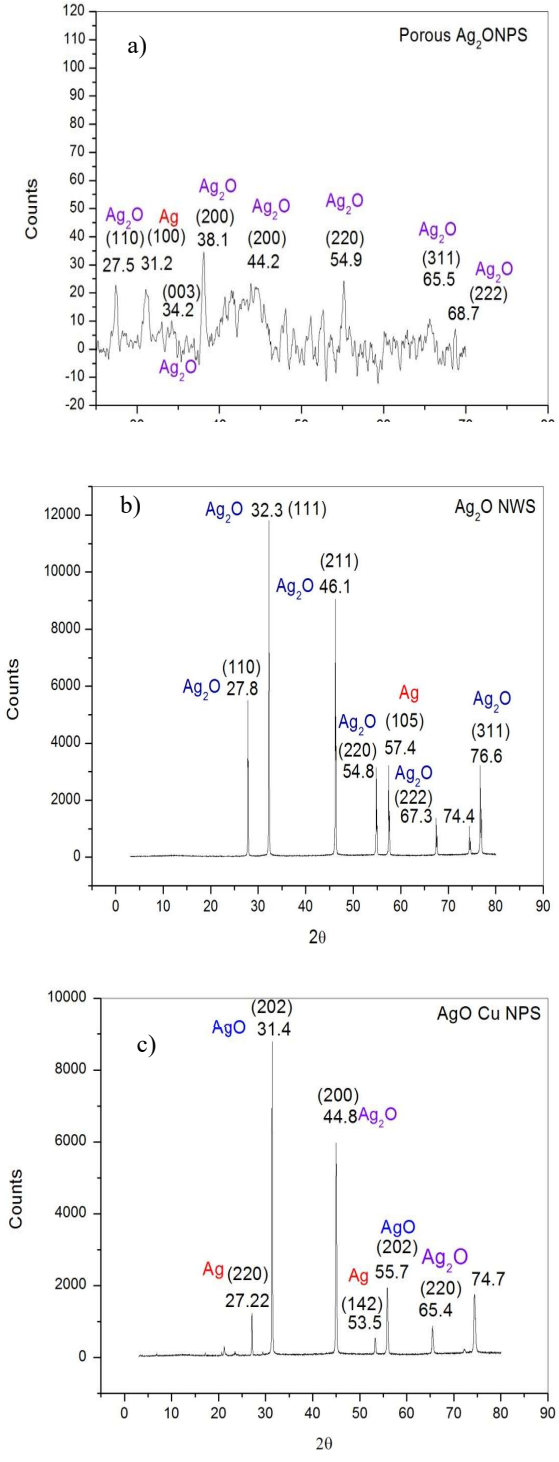

Fig. 5. XRD analysis performed for an AgO and Ag_2O synthesized sample from silver nitrate with PVP. a) Ag_2O porous nano flakes particles, b) nanowires of Ag_2O and c) AgO using Cu catalyst nanoparticle

diffraction angle (2θ) 27.5°, 34.2°, 38.1°, 44.2°,54.9°, 65.5° and 68.7° correspond to (110), (003), (200), (200), (220), (311) and (222) of Ag2O. One peak is observed at 31.2° correspond to (100) of Ag. These peaks confirm that, the sample mostly contains Ag_2O nanoparticles with tiny presence of Ag. Figure (5b) shows six peaks observed at 27.8°, 32.3°, 46.1°, 54.8°, 67.3° and 76.6° correspond to (110), (111), (211), (220),(222), (311) of Ag_2O. One peak is observed at 57.4° correspond to (105) of Ag.

These peaks confirm that, the sample mostly contains Ag_2O nanoparticles with tiny presence of Ag. Figure (5c) shows that, two peaks observed at 31.4° and 55.7° correspond to (202), (202) of AgO, two peaks observed at 44.8° and 65.4° correspond to (200) , (220) of Ag_2O and two peaks observed at 27.22° and 53.5° correspond to (220) ,(142) of Ag. One unknown peak (74.7°) was also observed [30-32].

3.5 Scanning electron microscope:

The morphological properties of the material were examined using the scanning electron microscopy (SEM) technique (SEM, Quanta FEG 250, FEI) [33]. The SEM images of silver oxide NPs are shown in Figure (6). The silver oxide NPs have crystalline nature, wires and porous shapes with varying sizes such that the particle sizes start varying from 55 nm. Porous structure of silver oxide nanoparticles is due to uniform oxidation of the surface.

3.6 Differential scanning calorimetry:

Crystallizing thermal behavior of dispersed silver oxide nanowires and nanoporous silver oxide in cholesteryl benzoate using differential scanning calorimetry (DSC) (SETRAM DSC-evo 131, scan rate 5 °C/min) researched by degree calculation. All calculations are applied to the second heating/cooling cycle.

The DSC shows that: 1) in case of AgO NPS doping in cholesteryl benzoate with initial mass: 6.1 (mg), in heating cycle phase transition start at temperature (103.5 and 134.5°C), peak maximum at 118.3°C, in cooling cycle phase transition start at temperature (158.1 and 125.9 °C), peak maximum at 140.5°C. 2) in case of AgO NWS doping in

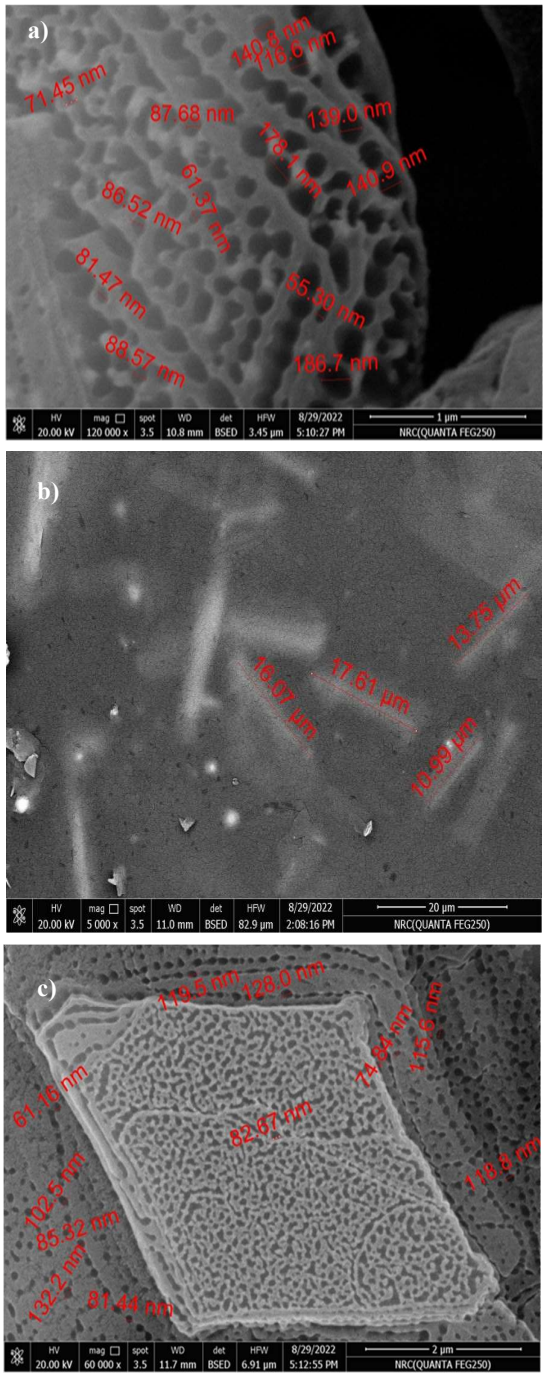

Fig. 6. SEM topography images of a) Ag NPs, b) Ag NWS and c) Ag Nps Cu

cholesteryl benzoate with initial mass: 5.9 (mg), in heating cycle phase transition start at temperature (98.7 and 129.9°C), peak maximum at 113.1°C, in cooling cycle phase transition start at temperature (158.6 and 122 °C),peak maximum at 138.3°C. 3) in

case of AgO NPS Cu doping in cholesteryl benzoate with initial mass: 7.3 (mg), in heating cycle phase transition start at temperature (107.2 and 138°C), peak maximum at 119.9°C, in cooling cycle phase transition start at temperature (157.7 and 126 °C), peak maximum at 141.7°C.

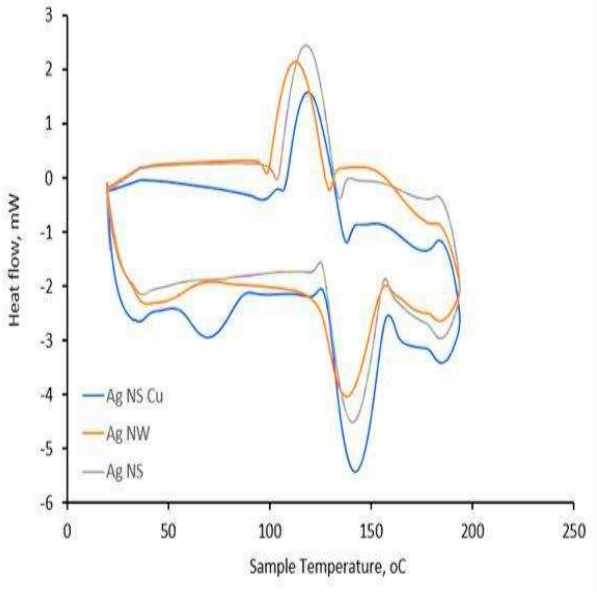

Fig.7. DSC of silver oxide nanoparticles in different forms.

Over all, there are a nice agreement between the phase detection by DSC and phase transition images with POM as confirmed tool with each other.

4. Conclusions:

This study successfully synthesized silver oxide nanowires and porous silver oxide nanoparticles capped with PVP and CTAB via hydrothermal and seed-mediate methods, respectively. Hydrothermal synthesis consists of the crystallization of nanoparticles at high temperatures and pressure in aqueous solution. Silver nanowires with lengths of 10-17µm, width 2.6-0.08 µm and porous silver nanoparticles with varying sizes such that the particle sizes start varying from 55 nm are produced. In addition, the synthesized silver oxide nanoparticles were mixed with cholesteryl benzoate liquid crystal, and the influence of the amount of silver oxide nanoparticles added was investigated. Analysis of the experimental data found that the physical characteristics of LC improve the dispersing of NPs.

The POM was in combination with a heating stage to evaluate the thermal stability of the cholesteryl benzoate liquid crystalline phase in the presence of metal nanoparticles. The presence of Silver oxide in different shape and size has a significant influence on the self-assemblies in cholesteryl benzoate which is consequences on main properties of CB such as texture and phase transition temperatures.

5. Conflicts of interest:

There is no conflicts of interest for this work.

6. Formatting of funding sources:

The authors would like acknowledge the project in house funding office at the National Research Centre, NRC, Egypt, for funding this work under project 13020227.

7. Acknowledgment:

Authors have a great thanks to nanomaterial investigation laboratory and liquid crystal laboratory, Central laboratories network, national research Centre for high and precision analysis and investigation of metal oxide nanomaterial and liquid crystals.

8. References

[1] S.H. Lee, B.-H. Jun, Silver nanoparticles: synthesis and application for nanomedicine, International journal of molecular sciences 20(4) (2019) 865. https://doi.org/10.3390/ijms20040865

[2] A. Syafiuddin, Salmiati, M.R. Salim, A. Beng Hong Kueh, T. Hadibarata, H. Nur, A review of silver nanoparticles: research trends, global consumption, synthesis, properties, and future challenges, Journal of

the Chinese Chemical Society 64(7) (2017) 732-756. https://doi.org/10.1002/jccs.201700067

[3] K.W. Shah, T. Xiong, Multifunctional metallic nanowires in advanced building applications, Materials 12(11) (2019) 1731. https://doi.org/10.3390/ma12111731

[4] L. Dai, C. Sow, C. Lim, V. Tan, Metal Oxide Nanowires–Structural and Mechanical Properties, Nanowires-Fundamental Research, IntechOpen 2011.

[5] R.A. Dorgham, M.N. Abd Al Moaty, K.P. Chong, B.H. Elwakil, Molasses-Silver Nanoparticles: Synthesis, Optimization, Characterization, and Antibiofilm Activity, International Journal of Molecular Sciences 23(18) (2022) 10243. https://doi.org/10.3390/ijms231810243.

[6] E. Abkhalimov, V. Ershov, B. Ershov, Determination of the concentration of silver atoms in hydrosol nanoparticles, Nanomaterials 12(18) (2022) 3091. https://doi.org/10.3390/nano12183091

[7] X.-F. Zhang, Z.-G. Liu, W. Shen, S. Gurunathan, Silver nanoparticles: synthesis, characterization, properties, applications, and therapeutic approaches, International journal of molecular sciences 17(9) (2016) 1534. https://doi.org/10.3390/ijms17091534

[8] S. Sahoo, A. Gopalan, S. Ramesh, P. Nirmala, G. Ramkumar, S. Agnes Shifani, R. Subbiah, J. Isaac JoshuaRamesh Lalvani, Preparation of polymeric nanomaterials using emulsion polymerization, Advances in Materials Science and Engineering 2021 (2021)1-9. https://doi.org/10.1155/2021/1539230

[9] S. Zeroual, P. Estellé, D. Cabaleiro, B. Vigolo, M. Emo, W. Halim, S. Ouaskit, Ethylene glycol based silver nanoparticles synthesized by polyol process: Characterization and thermophysical profile, Journal of Molecular Liquids 310 (2020) 113229. https://doi.org/10.1016/j.molliq.2020.113229

[10] G. Cordoyiannis, M. Lavrič, V. Tzitzios, M. Trček, I. Lelidis, G. Nounesis, S. Kralj, J. Thoen, Z. Kutnjak, Experimental advances in nanoparticle-driven stabilization of liquid-crystalline blue phases and twist-grain boundary phases, Nanomaterials 11(11) (2021) 2968. https://doi.org/10.3390/nano11112968.

[11] 11. M. Jasiurkowska-Delaporte, Ł. Kolek, Nematic Liquid Crystals, Crystals, 2021, 11, p. 381. https://doi.org/10.3390/cryst11040381M.

[12] A. Liang, Y. Shu, S. Zhi, Z. Jiang, A new aptamer SERSquantitative platform for ultratrace Pb (II) based on cholesterol benzoate liquid crystal loaded-

nanosilvercatalytic amplification, Available at SSRN 4062791. http://dx.doi.org/10.2139/ssrn.4062791.

[13] C.F. Dietrich, Lyotropic nematic liquid crystals: interplay between a small twist elastic constant and chirality effects under confined geometries, Liquid Crystals Today 30(1) (2021) 2-14. https://doi.org/10.1080/1358314X.2021.1928961

[14] Y. Saadat, O.Q. Imran, C.O. Osuji, R. Foudazi, Lyotropic liquid crystals as templates for advanced materials, Journal of Materials Chemistry A 9(38) (2021) 21607-21658. https://doi.org/10.1039/D1TA02748D

[15] C.F. Dietrich, P. Rudquist, P.J. Collings, F. Giesselmann, Interplay between confinement, twist elasticity, and intrinsic chirality in micellar lyotropic nematic liquid crystals, Langmuir 37(8) (2021) 2749-2758. https://doi.org/10.1021/acs.langmuir.0c03500.

[16] V.P. Chavda, S. Dawre, A. Pandya, L.K. Vora, D.H. Modh, V. Shah, D.J. Dave, V. Patravale, Lyotropic liquid crystals for parenteral drug delivery, Journal of Controlled Release 349 (2022) 533-549. https://doi.org/10.1016/j.jconrel.2022.06.062

[17] A. Rodriguez-Palomo, V. Lutz-Bueno, M. Guizar-Sicairos, R. Kádár, M. Andersson, M. Liebi, Nanostructure and anisotropy of 3D printed lyotropic liquid crystals studied by scattering and birefringence imaging, Additive Manufacturing 47 (2021) 102289. https://doi.org/10.1016/j.addma.2021.102289

[18] A. Shete, S. Nadaf, R. Doijad, S. Killedar, Liquid Crystals: Characteristics, Types of Phases and Applications in Drug Delivery, Pharmaceutical Chemistry Journal 55 (2021) 106-118. https://doi.org/10.1007/s11094-021-02396-y

[19] A.M. Labeeb, Y.A. Ward, M. Fikry, Thermal control of tunable photonic optical bandgaps in different cholesteric liquid crystals mixtures, Journal of Molecular Liquids 340 (2021) 117179. https://doi.org/10.1016/j.molliq.2021.11717920.

[20] C.Y. Liu, C.C. Chen, C.M. Tu, S.C. Hung, C.H. Chao, Structure colorants based on cross-linked cholesteric liquid crystalline polymeric slices, Journal of Applied Polymer Science 139(8) (2022) 51717. https://doi.org/10.1002/app.5171721.

[21] Y. Yang, D. Zhou, X. Liu, Y. Liu, S. Liu, P. Miao, Y. Shi, W. Sun, Optical fiber sensor based on a cholesteric liquid crystal film for mixed VOC sensing, Optics Express 28(21) (2020) 31872-31881. https://doi.org/10.1364/OE.405627.

[22] S. Warsi, R. Manohar, Principal Polarizability and Orientational Order

Parameter Study of some Pure Cholesteric Liquid Crystals and their Homogeneous Mixtures: Phase Transition Behaviour, Indian Journal of Science and Technology 15(31) (2022) 1541-1547. https://doi.org/10.17485/IJST/v15i31.1084.

[23] T. Sarukhanyan, The Polarization of Laser Generation from the Cholesteric Liquid Crystal–Dye-Doped Polymer Layer–Cholesteric Liquid Crystal System, Journal of Contemporary Physics (Armenian Academy of Sciences) 56(2) (2021) 103-108. https://doi.org/10.3103/S1068337221020146.

[24] A.M. Labeeb, A.A. Ward, S. Ibrahim, F. Fouad, R.M. Ramadan, Novel nanocomposites based on Tetrazine liquid crystals for energy storage application, Journal of Molecular Liquids 392 (2023) 123495. https://doi.org/10.1016/j.molliq.2023.123495.

[25] A. Labeeb, S. Ibrahim, A. Ward, S. Abd-El-Messieh, Polymer/liquid crystal nanocomposites for energy storage applications, Polymer Engineering & Science 60(10) (2020) 2529-2540. https://doi.org/10.1002/pen.25491

[26] J. Prakash, S. Khan, S. Chauhan, A. Biradar, Metal oxide-nanoparticles and liquid crystal composites: A review of recent progress, Journal of Molecular Liquids 297 (2020) 112052. https://doi.org/10.1016/j.molliq.2019.112052

[27] A. Kumar, M.O. Shaikh, C.-H. Chuang, Silver nanowire synthesis and strategies for fabricating transparent conducting electrodes, Nanomaterials 11(3) (2021) 693. https://doi.org/10.3390/nano11030693

[28] S. Hemmati, M.T. Harris, D.P. Barkey, Polyol silver nanowire synthesis and the outlook for a green process, Journal of Nanomaterials 2020 (2020) 1-25. https://doi.org/10.1155/2020/9341983

[29] S. Ibrahim, K.M. El-Khawas, Development of eco-environmental nano-emulsified active coated packaging material, Journal of King Saud University-Science 31(4) (2019) 1485-1490. https://doi.org/10.1016/j.jksus.2019.09.010.

[30] S. Vinay, Udayabhanu, H. Sumedha, G. Nagaraju, S. Harishkumar, N. Chandrasekhar, Facile combustion synthesis of Ag_2O nanoparticles using cantaloupe seeds and their multidisciplinary applications, Applied Organometallic Chemistry 34(10) (2020) e5830. https://doi.org/10.1002/aoc.5830

[31] A. Rita, A. Sivakumar, S.S.J. Dhas, S.M.B. Dhas, Structural, optical and

magnetic properties of silver oxide (AgO) nanoparticles at shocked conditions, Journal of Nanostructure in Chemistry 10 (2020) 309-316. https://doi.org/10.1007/s40097-020-00351-z

[32] A.A. Fayyadh, M.H. Jaduaa Alzubaidy, Green-synthesis of Ag2O nanoparticles for antimicrobial assays, Journal of the Mechanical Behavior of Materials 30(1) (2021) 228-236. https://doi.org/10.1515/jmbm-2021-0024

[33] H. Abdolmohammad-Zadeh, E. Rahimpour, S. Bahramzadeh, An Innovative Nanosorbent Based on ZnO@ Ag2O@ Fe3O4 Nanocomposite-for Extraction and Preconcentration of Cd (II) Ions from Water Samples, Analytical and Bioanalytical Chemistry Research 5(2) (2018) 229-247. https://doi.org/10.22036/ABCR.2018.125442.1197.